

Assessment of *pre-crisis* and *syn-crisis* seismic hazard at Campi Flegrei and Mt. Vesuvius volcanoes, Campania, southern Italy

Vincenzo Convertito · Aldo Zollo

Received: 17 March 2010 / Accepted: 11 January 2011
© Springer-Verlag 2011

Abstract In this study, we address the issue of short-term to medium-term probabilistic seismic hazard analysis for two volcanic areas, Campi Flegrei caldera and Mt. Vesuvius in the Campania region of southern Italy. Two different phases of the volcanic activity are considered. The first, which we term the *pre-crisis* phase, concerns the present quiescent state of the volcanoes that is characterized by low-to-moderate seismicity. The second phase, *syn-crisis*, concerns the unrest phase that can potentially lead to eruption. For the Campi Flegrei case study, we analyzed the pattern of seismicity during the 1982–1984 ground uplift episode (bradyseism). For Mt. Vesuvius, two different time-evolutionary models for seismicity were adopted, corresponding to different ways in which the volcano might erupt. We performed a site-specific analysis, linked with the hazard map, to investigate the effects of input parameters, in terms of source geometry, mean activity rate, periods of data collection, and return periods, for the *syn-crisis* phase. The analysis in the present study of the *pre-crisis* phase allowed a comparison of the results of probabilistic seismic hazard analysis for the two study areas with those provided in the Italian national hazard map. For the Mt. Vesuvius

area in particular, the results show that the hazard can be greater than that reported in the national hazard map when information at a local scale is used. For the *syn-crisis* phase, the main result is that the data recorded during the early months of the unrest phase are substantially representative of the seismic hazard during the whole duration of the crisis.

Keywords Seismic hazard · Unrest phase · Ground-motion attenuation · Uniform hazard spectra

Introduction

Seismicity occurring in volcanic areas is generally characterized by earthquakes for which the frequency of occurrence and magnitude values mainly depend on the unrest state of the volcano, the location and upward migration of magma, the hydrothermal fluid circulation, the induced fracturing phenomena, and the local stress variations. Volcanic risk is the main concern for volcanic areas, and patterns of seismicity can be analyzed and used to underpin long-range and short-range forecasts (Newhall 2009). In highly densely populated areas, however, seismicity can represent a threat for the inhabitants and for the civil structures and industrial facilities in the area. This is the case for the two main volcanic areas considered here, Campi Flegrei caldera and Mt. Vesuvius, in the Campania region of southern Italy, for which the estimates of seismic hazard can be used to reduce the impact of any earthquakes occurring before and during the unrest phase.

Campi Flegrei is an active volcanic area that is located west of the city of Naples, and which covers an area of about 400 km². The last eruption, which occurred in 1538, produced a small, about 100-m-high cone, called Mt. Nuovo.

Editorial responsibility: M. Ripepe

V. Convertito (✉)
Istituto Nazionale di Geofisica e Vulcanologia, Osservatorio
Vesuviano (INGV),
Via Diocleziano 328,
80124 Naples, Italy
e-mail: vincenzo.convertito@ov.ingv.it

A. Zollo
Dipartimento di Scienze Fisiche, Università di Napoli Federico II,
Via Cintia,
80125 Naples, Italy

Seismic activity was noted at least 40 years before this eruption, with a noticeable increase in activity during the 2 years preceding this event. More recently, two main ground uplift episodes have taken place within the caldera: in 1970–72 and 1982–84. These were accompanied by intense microseismic activity. In the period of September 1970 to September 1972, three thousand shallow micro-earthquakes were recorded by a local network that consisted of five to seven stations (Corrado et al. 1976). A slight subsidence occurred in the period 1972–1974, and then the ground remained approximately at the same level until May–June 1982. At this point, the ground started to rise again at a very high rate (2 mm per day on average). An anomalous increase in seismic activity was observed a few months after the onset of this last uplift (Del Pezzo et al. 1984). More than 10,000 shallow-depth micro-earthquakes with magnitudes <4.2 were recorded from October 1982 to September 1984. The persistent seismic activity and the structural failure of buildings that resulted from a total 1.8 m uplift of the ground led the local authorities to evacuate large districts of the town of Pozzuoli, near the coast.

Our other study site, Mt. Vesuvius, has been quiescent since the last eruption, which occurred in 1944. It is one of the most dangerous volcanoes in the world, because more than 700,000 people live in close proximity to the crater. The volcano's present state is characterized by a low level of seismicity (a few hundreds microearthquakes per year), with most of the earthquakes having a local magnitude, $M_L < 3.0$. The earthquakes are mainly located

beneath the crater area at very shallow depths (less than 5 km). The strongest earthquake occurred on October 9, 1999 (M_L 3.6), and it was clearly felt in the area surrounding the volcano and in the city of Naples, creating panic among the population and attracting much media attention.

Due to the lack of instrumental data relating to past eruptions and the accompanying seismicity, no consensus exists about the expected maximum magnitude values and frequency of earthquake occurrence for these two areas. Frequent, shallow low-magnitude earthquakes can, however, have an important influence in seismic hazard analysis, particularly over intermediate and long return periods (Reiter 1990). Indeed, although low magnitude earthquakes ($M < 5.0$) rarely produce structural damage, they can generate panic and can cause damage to non-structural components of buildings such as parapets, architectural decorations, chimneys, partition walls, ceiling panels, windows, light fixtures, and building contents (Chen and Scawthorn 2003).

For such minor damage, the application and the results of a probabilistic seismic hazard analysis (PSHA) can be used as input by engineers to calculate damage probability using vulnerability data, which will be useful for the planning of operations during any emergency. Indeed, due to its probabilistic nature, PSHA can be used both to test *a-priori* hypotheses of the seismicity and its time evolution, and to compute the effects of these assumptions in terms of probability of exceedance of a set of strong ground-motion parameters. As reported in the building codes, (e.g., Eurocode 8—CEN 2003), these parameters represent the

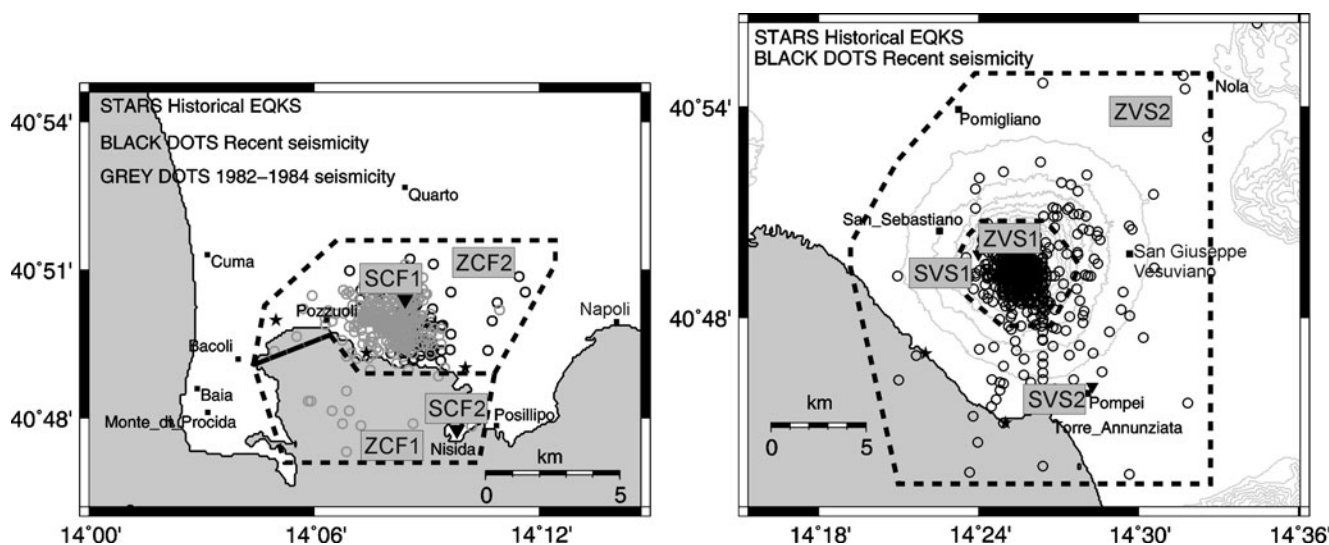
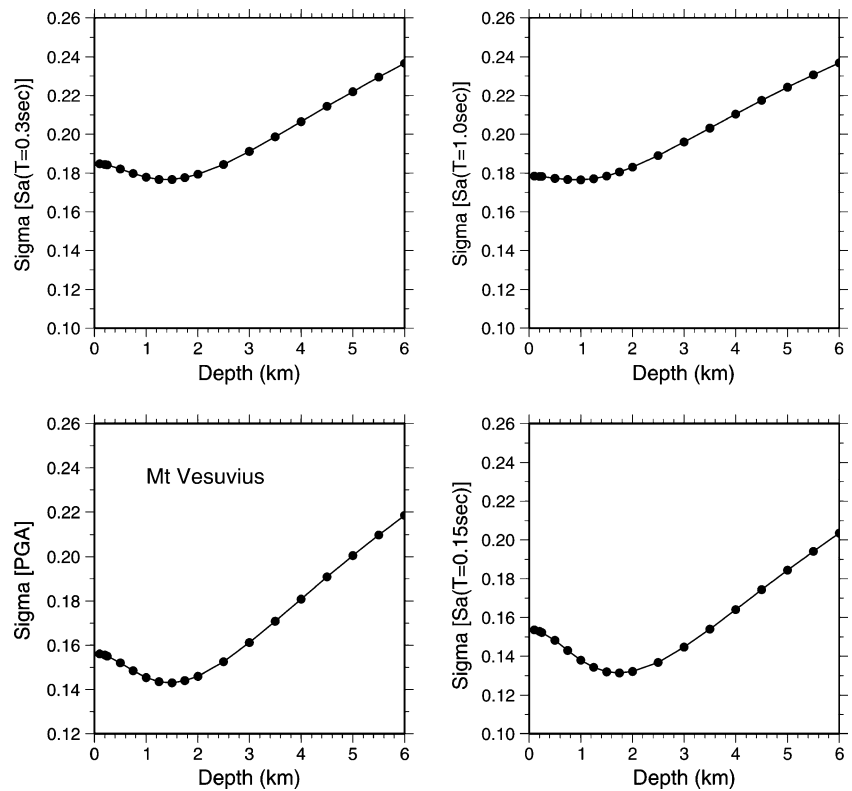


Fig. 1 Earthquake source areas. *Left panel*, Campi Flegrei area. *Right panel*, the Mt. Vesuvius area. *Dashed lines*, perimeter of the earthquake sources. *Circles*, recent seismicity. *Stars*, historical earthquakes retrieved from the CPTI04 catalogue, provided by the Gruppo

di lavoro CPTI (2004) restricted to the area of interest. *Grey dots* (*left panel*), 1982–1984 crisis. Sites used for site-specific PSHA are also reported

Fig. 2 Minimization of standard error for estimating the h parameter for the Mt. Vesuvius area and for all of the spectral ordinates considered



information that will be used to design new structures and to perform retrofit analyses of existing structures.

In the present study, a new technique to calculate PSHA for rock-site conditions is proposed for the Campi Flegrei and Mt. Vesuvius areas. Specifically, the new technique considers two phases: the *pre-crisis* period, corresponding to a time interval during which no potentially precursory phenomena are observed, and the *syn-crisis* period, corresponding to the time interval preceding a ‘probable’ eruption (also termed the unrest phase) during which potentially precursory phenomena are observed. For the *pre-crisis* phase, the classical approach for PSHA proposed by Cornell (1968) has been applied, and hazard maps for Peak Ground Acceleration (PGA) and two return periods of 475 year and 975 year have been calculated. For the seismic hazard during the *syn-crisis* phase for the

Campi Flegrei area, we considered the seismic activity that occurred during the 1982–1984 bradyseism. Similarly, for the Mt. Vesuvius area, we assigned the *syn-crisis* phase a total duration of 2 years based on the duration of precursors to the 1944 eruption, while for the *b*-value of the Gutenberg-Richter (GR) relationship (Gutenberg and Richter 1944), two distinct trends were considered, characterized by an increasing and a decreasing *b*-value with time. In this way, two different modalities of seismicity occurrence were investigated, both of which were associated with a frequency magnitude distribution that can, but does not always, lead to eruption. For example, the seismic activity preceding the eruption of Mt. St. Helens on 18 May 1980 was characterized by increasing seismic energy and a decrease in the *b*-value as the time of eruption approached (Qamar et al. 1983). In

Table 1 Regression coefficients of Eq. 1 for Sa(T) relative to the Campi Flegrei area

Sa(T) (m/s ²)	a	b	c	h	σ
Sa(T=0 s)	-4.163	0.967	-1.572	1.00	0.181
Sa(T=0.15 s)	-3.560	0.904	-1.629	1.25	0.188
Sa(T=0.3 s)	-4.303	1.063	-1.511	1.00	0.194
Sa(T=1.0 s)	-6.129	1.317	-1.401	1.00	0.105

Table 2 Regression coefficients of Eq. 1 for Sa(T) relative to the Mt. Vesuvius area

Sa(T) (m/s ²)	a	b	c	h	σ
Sa(T=0 s)	-2.899	0.741	-1.816	1.5	0.143
Sa(T=0.15 s)	-2.291	0.682	-1.969	1.75	0.131
Sa(T=0.3 s)	-2.928	0.800	-1.690	1.5	0.177
Sa(T=1.0 s)	-4.953	1.100	-1.354	1.0	0.176

Fig. 3 Ground motion prediction equation for the Campi Flegrei and Mt. Vesuvius areas *Lower panels*, the Campi Flegrei area. *Upper panels*, Mt. Vesuvius area. *Dots*, simulated stochastic ground-motion values. *Continuous black lines*, best-fit curves for magnitude values ranging from 2.0 to 5.0

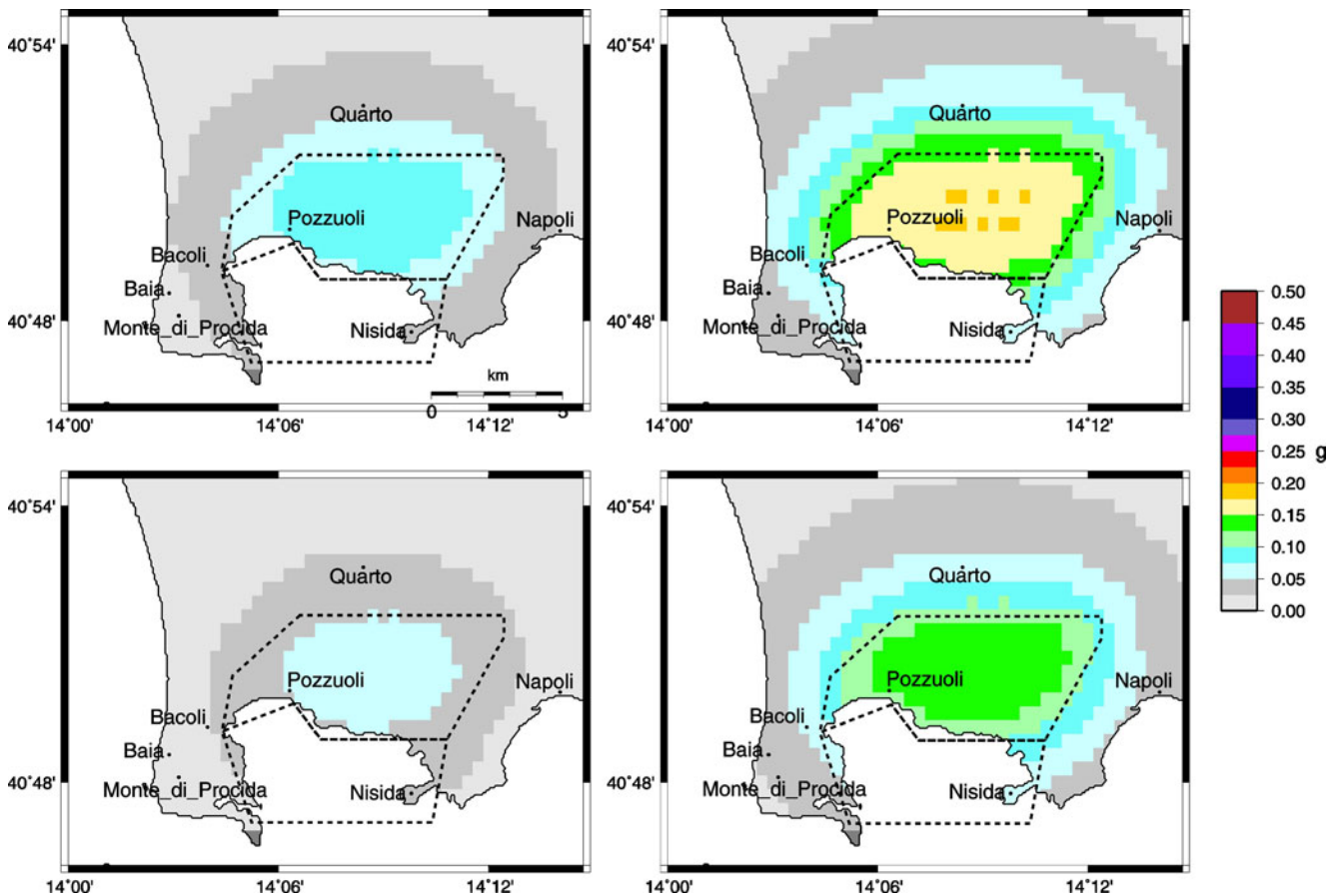
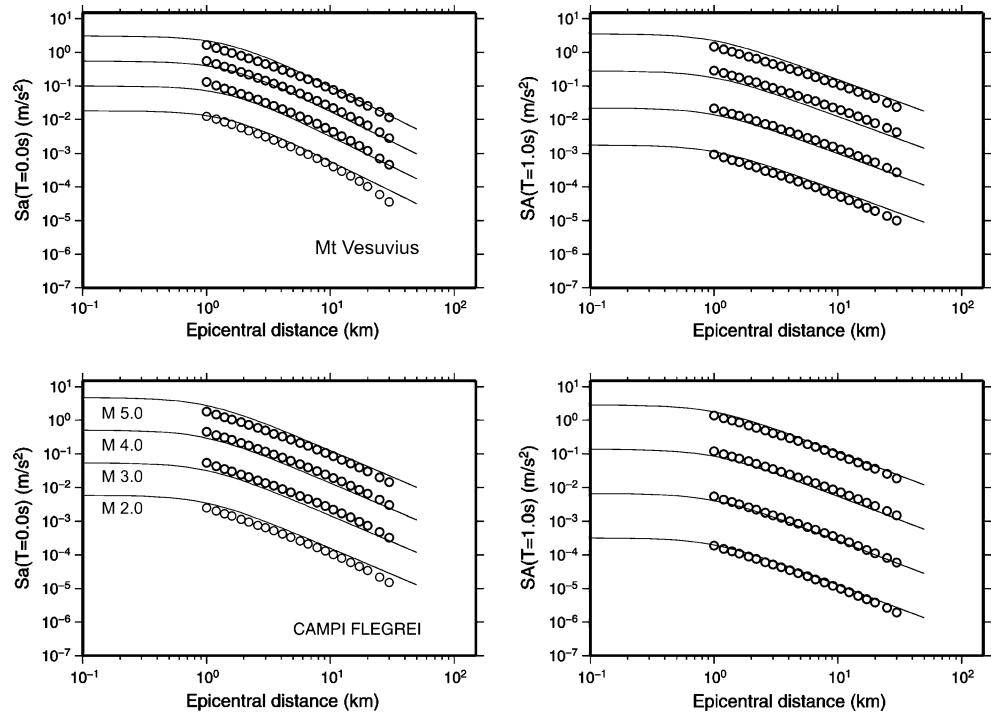


Fig. 4 Hazard maps for PGA in unit of g for 475-year and 975-year return periods. *Left panels*, case #1, where a 400-year completeness period was assumed for the national seismic catalog. *Right panels*,

case #2, where the Italian ZS9 seismic zoning is referred to (Meletti et al. 2008). *Lower panels*, 475-year return period. *Upper panels*, 975-year return period

contrast, for some other volcanoes (e.g., Mt. Spurr, Alaska, 1992; Mt Etna, Italy, 1981), an increase in b -value has been seen prior to major eruptions (e.g., Endo et al. 1981; De Natale et al. 1986).

In addition, the uniform hazard spectra (UHSs) for two sites located in different positions with respect to the seismic source zones were computed for the *syn-crisis* analysis. With the hypothesis that from a dynamic point of view, an engineering structure can be idealized as an elastic-damped, single-degree-of-freedom system with a given natural period of vibration, for a given probability of exceedance, the UHS provides the variation of the peak values of ground motion as a function of the natural period. These spectra allow calculation of the effects of ongoing seismicity on structures characterized by different natural elastic periods. We investigated the spectra at the zero-frequency asymptote, which corresponds to the PGA, at 0.15 s, 0.3 s and 1.0 s.

Probabilistic seismic hazard analysis

For any selected site, PSHA furnishes a hazard curve that represents the probability of exceedance of the ground-motion parameter, A , in a given time interval; as for example, during the design life of a building, a bridge or other infrastructure. The computation of the hazard curve requires computation of the hazard integral (Cornell 1968; Bazzurro and Cornell 1999) that for the i -th

selected earthquake source zone and for a range of possible magnitudes and distances, provides the mean annual rate of exceedance, as in the following equation:

$$E_i(A > A_0) = \alpha_i \int_M \int_R \int_s I[A > A_0 | m, r, \varepsilon] f(m) f(r) f(\varepsilon) dm dr d\varepsilon \tag{1}$$

where I is an indicator function that equals 1 if A is larger than A_0 for a given distance r , ranging between R_{\min} and R_{\max} , a given magnitude m , ranging between M_{\min} and M_{\max} , and a given ε , which represents the residual variability of the A parameter with respect to the selected Ground Motion Prediction Equation (GMPE) (e.g., Bazzurro and Cornell 1999), which expresses the variation of the strong ground-motion parameter as a function of the source-to-site distance and magnitude of the earthquake. The probability density functions (PDFs) for M , $f(m)$, and for R , $f(r)$, depend on the adopted earthquake recurrence model (e.g., Gutenberg and Richter 1944), and on the site location and source geometry, respectively. Finally, α_i for each identified source represents the mean annual rate of occurrence of the earthquakes within the source retrieved from the seismic catalogs. Given the magnitude and the distance, ε is defined as the number of logarithmic standard deviations by which the logarithm ground motion deviates from the median. Thus, via its associated PDF, $f(\varepsilon)$, it allows incorporation of the residual variability of the

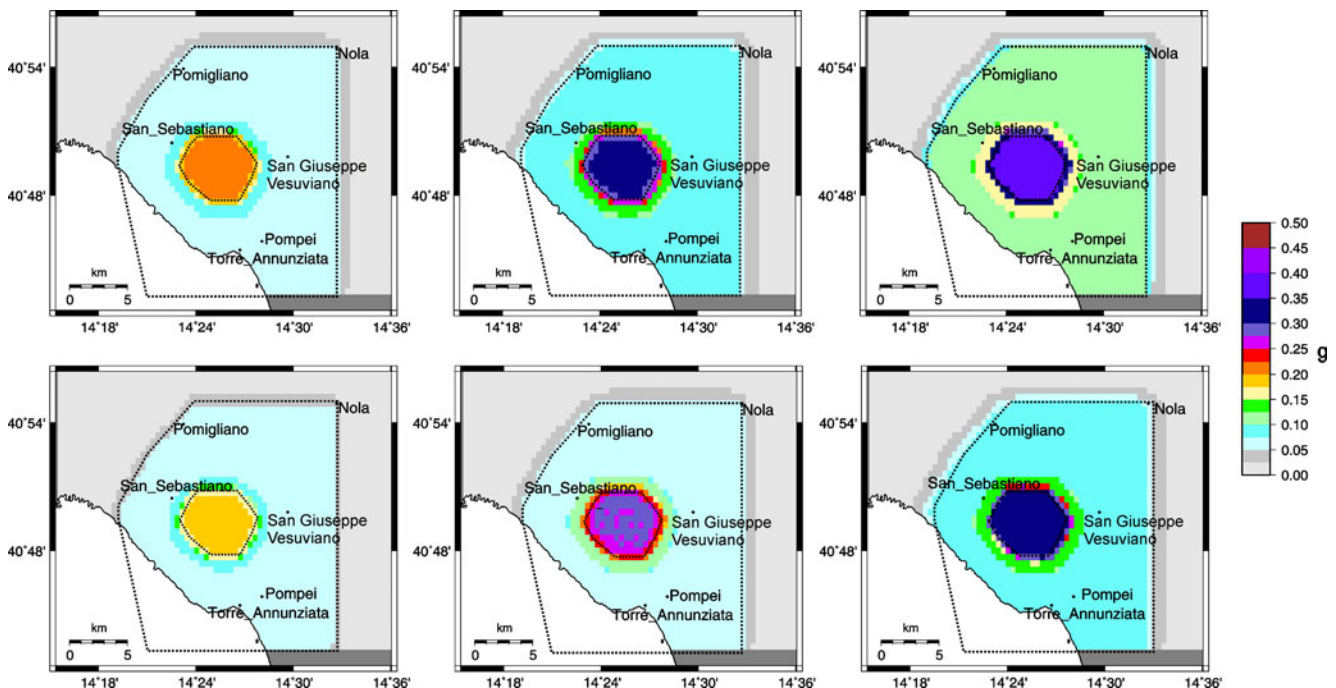


Fig. 5 Hazard maps for PGA expressed in unit of g for the *pre-crisis* phase and three b -values. *Left panel*, $b=2.3$. *Central panel*, $b=1.6$. *Right panel*, $b=1.1$. *Lower panels*, 475-year return period. *Upper panels*, 975-year return period

ground-motion parameter for which the hazard is estimated (e.g., Bazzurro and Cornell 1999).

Assuming a homogeneous Poissonian recurrence model, for a given site, Eq. 1 allows the probability of exceedance P in a time interval t to be computed:

$$P(A > A_0, t) = 1 - e^{-\sum_{i=1}^N E_i(A > A_0) \cdot t} \quad (2)$$

where the sum is taken over all of the sources that contribute to the hazard. When the analysis is performed for a set of sites covering an area of interest, with the exposure time fixed, (~50 years for civil structures) and the probability of exceedance (10%), a hazard map can be produced (Reiter 1990; Giardini 1999).

In the following sections, the procedure implemented to perform PSHA analysis at Campi Flegrei and Mt. Vesuvius is described. In particular, using the historical seismic catalog of Italy (*Catalogo Parametrico dei Terremoti Italiani*, CPTI04 catalog, Gruppo di lavoro CPTI 2004) limited to the area of interest, along with the location of the recent instrumental seismicity provided by Istituto Nazionale di Geofisica e Vulcanologia (INGV)—Osservatorio Vesuviano (<http://www.ov.ingv.it>), *ad-hoc* earthquake source zones for these two areas were identified. GMPEs that are expected to greatly affect the results of the analysis were retrieved for the two areas separately, to allow for the differences in static stress-drop conditions and anelastic attenuation.

The hazard maps for the PGA for two return periods, 475 year and 975 year, were calculated for the *pre-crisis* phase. For the Mt. Vesuvius area, different seismic hazard maps were computed by changing the b -value of the GR relationship and the value of the mean seismicity rate. Following De Natale and Zollo (1986), PSHA for the *syn-crisis* phase was performed assuming that the pre-eruptive seismicity was characterized by a swarm-like behavior with clusters of microearthquakes, the number of which followed a Poissonian distribution as a function of time. Thus, given an observation period during which potentially precursory phenomena were observed, peak ground-motion values with a selected return period were computed. Specifically, during the observation period, the mean activity rate, the number of earthquakes, and the b -value can be calculated and used as input parameters for PSHA, which is calculated for return periods of 6, 12, 18 and 24 months.

Seismic sources identification

As reported in the pioneering study by Cornell (1968), PSHA first requires identification of the earthquake sources

based on the geological, tectonic and seismic data that are available for the study areas. The source areas can range from well-known and localized faults, to entire seismotectonic provinces that extend for thousands of square kilometers. The configuration of the single source can be a point, a line, an area or a volume.

For both the Campi Flegrei and Mt. Vesuvius areas, the earthquake sources were defined based on the

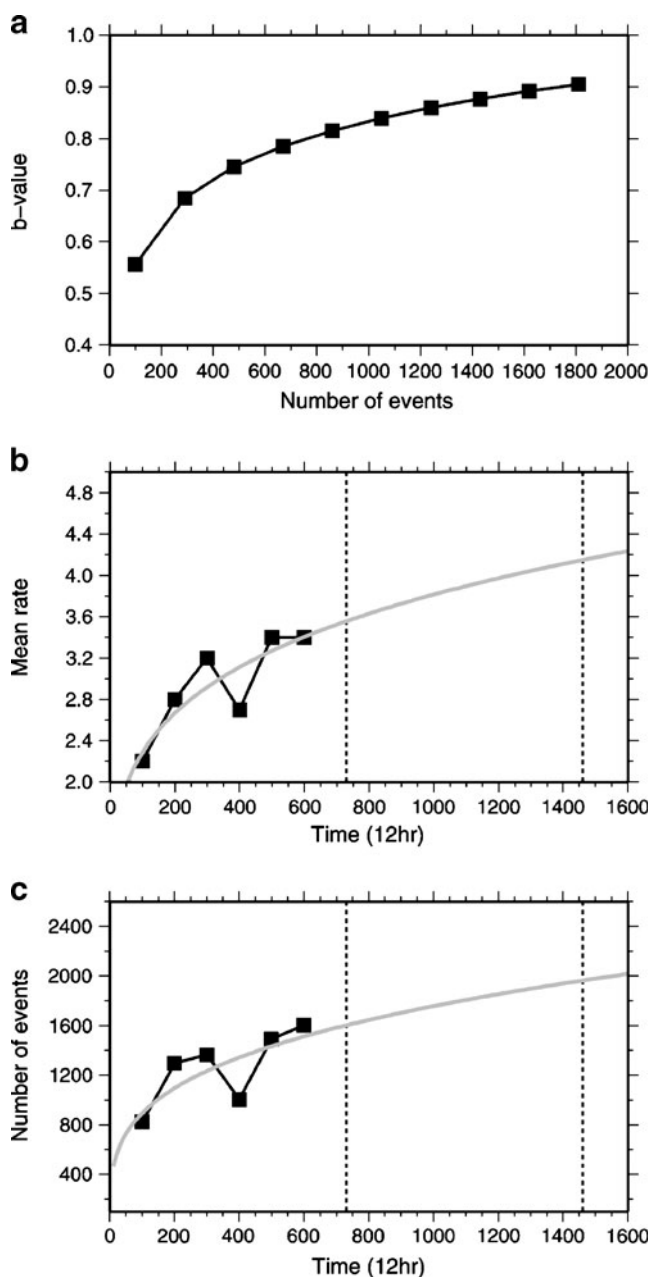


Fig. 6 Retrieved model for seismicity characterizing the Campi Flegrei area during the *syn-crisis* phase. *Black dots*, data retrieved from De Natale and Zollo (1986). *Continuous lines*, the models in Eqs. 4 and 5

location of both of the historical earthquakes and instrumental seismicity. Moreover, for the Campi Flegrei area, the location of the earthquakes that occurred during the 1982–1984 crisis were also used (Battaglia et al. 2008). With the aim of accounting for the spatial differences in the earthquake occurrence for both of the investigated areas, an additional separation was performed. Looking at the earthquake locations (Fig. 1), for the two volcanoes, two separate zones can be identified. One is characterized by a rather sparse distribution, which is thus considered as a background zone dominated by tectonic events, while the other is characterized by a more dense and quite uniform distribution. The two areas are indicated as ZCF1 and ZCF2 for Campi Flegrei caldera, and ZVS1 and ZVS2, for Mt. Vesuvius (Fig. 1).

Ground-motion prediction equations for the Campi Flegrei and Mt. Vesuvius areas

To estimate the effects of the selected earthquakes, the GMPEs were retrieved for spectral ordinates $S_a(T)$ at structural periods $T=0.0, 0.15, 0.3$ and 1.0 s, which correspond to the natural period of oscillation of the engineering structures considered. Due to the lack of experimental data from moderate-to-large earthquakes, a database of synthetic data was computed using the stochastic ground motion simulation approach proposed by Boore (1983) for both Campi Flegrei and Mt. Vesuvius. The static stress drop ($\Delta\sigma$) and anelastic attenuation parameters (Q) were retrieved from De Natale et al. (1987) for the Campi Flegrei area, and from Galluzzo et al. (2009) for the Mt. Vesuvius area.

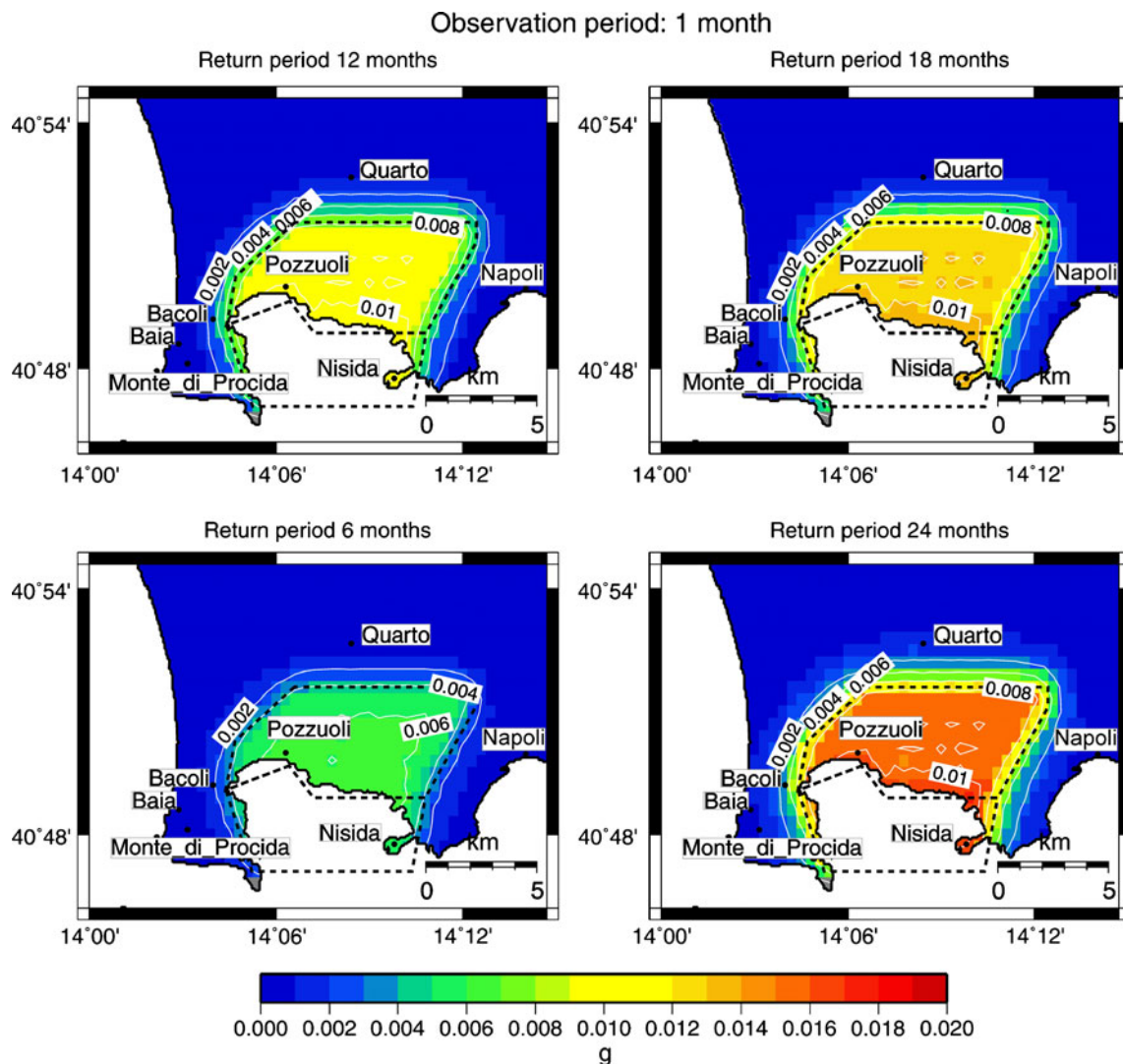


Fig. 7 Hazard maps for PGA in units of g for the *syn-crisis* phase of the Campi Flegrei area relative to the 1-month observation period and four return periods expressed in months selected on the basis of the assumed 24 months duration of the *syn-crisis* phase

Specifically, for the Campi Flegrei area, $\Delta\sigma=40$ bars, $Q(f)=98f^{0.43}$ and $\kappa=0.015$ s⁻¹, whereas for the Mt. Vesuvius area, $\Delta\sigma=10$ bars and $Q=150$. As described by Anderson and Hough (1984), the κ parameter governs the high-frequency (larger than 2 Hz) spectral decay that is mainly caused by subsurface geological structures near to the site. Simulated data were used to fit Eq. 3 (e.g., Sabetta and Pugliese 1996; Ambraseys et al. 1996):

$$\log S_a(T) = a + bM + c \log \sqrt{R^2 + h^2} \pm \sigma_{\log S_a(T)} \quad (3)$$

where M is magnitude, R is the epicentral distance in km. The parameter h represents a fictitious depth used to avoid ground-motion saturation with distance (e.g., Campbell 1981; Sabetta and Pugliese 1996). The best

value for h was retrieved by minimizing the standard error $\sigma_{\log S_a(T)}$. To do this, a set of 18 values of h was selected, and for each of them, the regression was performed. The best h value thus corresponded to the minimum value of $\sigma_{\log S_a(T)}$. As an example, Fig. 2 shows the results of the procedure described above for the area of Mt. Vesuvius.

The best-fit coefficients and standard errors for the selected spectral ordinates are listed in Table 1 for Campi Flegrei and in Table 2 for the Mt. Vesuvius area, while Fig. 3 shows the simulated data and the retrieved GMPEs for four magnitude values. It is worth noting the differences in attenuation for the two areas, and importantly, that low magnitude events can also result in high $S_a(T)$ values, due to the small distance range. This has direct implications for seismic hazard in the areas considered.

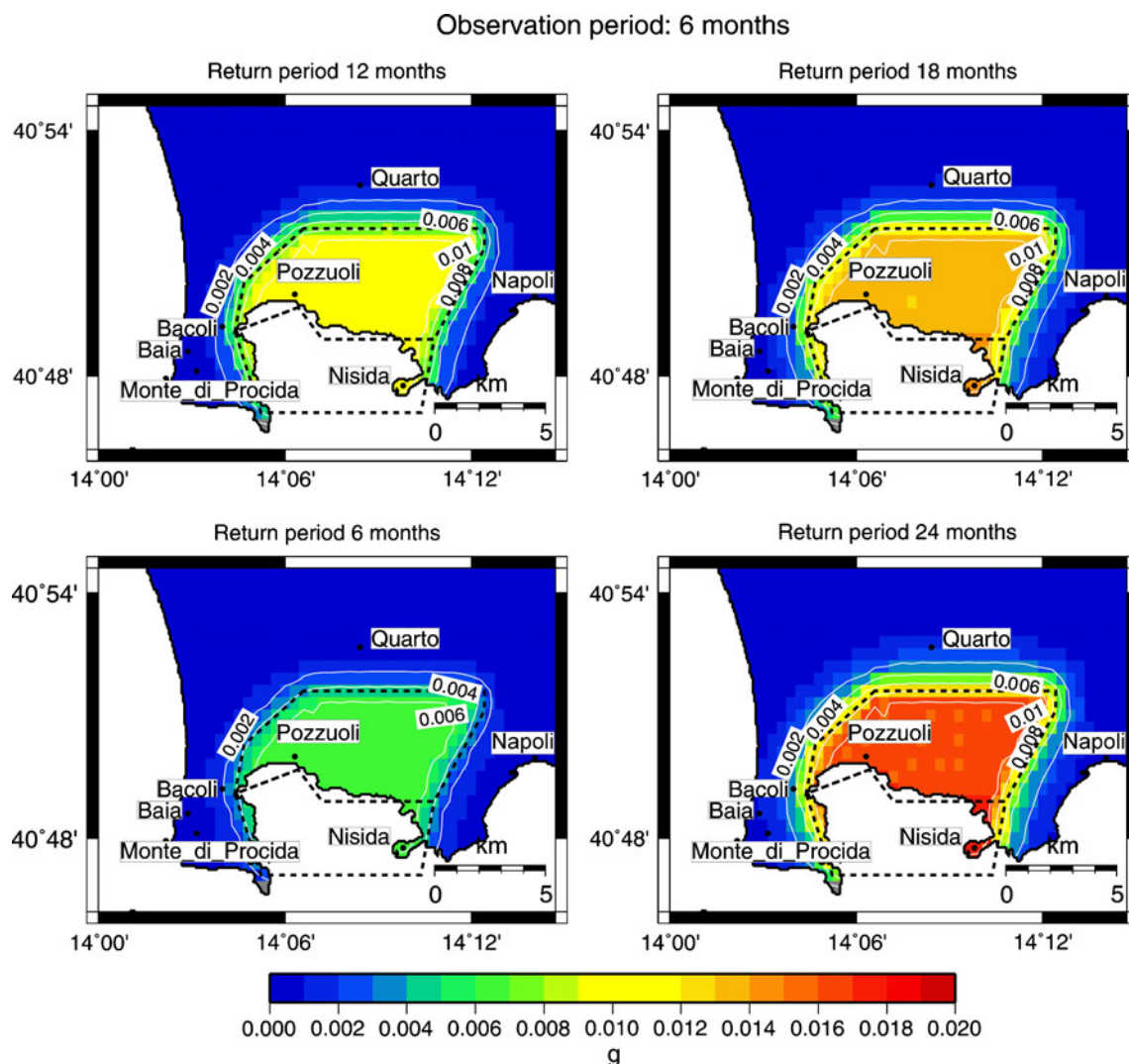


Fig. 8 As for Fig. 7, but for 6 months of observation period

Probabilistic seismic hazard analysis for the *pre-crisis* and *syn-crisis* phases

In the present study, PSHA is performed for two phases of interest, corresponding to our two states of the volcanoes, i.e., *pre-crisis* and *syn-crisis*. For both phases, the earthquake source zones identified were assumed to be characterized by uniform seismic potential (e.g., Reiter 1990). A homogeneous Poissonian recurrence model was assumed in the *pre-crisis* phase, while a generalized Poissonian model that allowed for time-dependent mean activity rates was used for PSHA during the *syn-crisis* phase. The following sections illustrate how the mean activity rates, the *b*-values of the GR relationship, and the maximum magnitude were selected for each area of interest.

Pre-crisis phase

Results for the Campi Flegrei area

To account for epistemic uncertainty relating to the mean activity rate, two different cases were considered. The first (case #1) corresponds to the case where a 400 year completeness period is assumed for the national seismic catalog (i.e., over 400 years, the earthquakes with magnitude in the range of interest occurred in the area under study are fully reported in the catalog). Four historical earthquakes (1198, Mw 5.17; 1538, Mw 5.37; 1582, Mw 5.37; and 1832, Mw 4.83) located in the area (Fig. 1, stars) were selected from the CPTI04 catalog (Gruppo di Lavoro CPTI 2004). Based on these assumptions, a mean activity rate $\alpha_2=0.01$ events/year was assigned to ZCF2, while for ZCF1 it was assumed that the activity rate was $\alpha_1=\alpha_2/2$. Moreover, a *b*-value of the GR relationship of 0.3 that was calculated from the available data was used for both zones.

In the second case (case #2), the Italian ZS9 seismic zoning was that of Meletti et al. (2008). In particular, the *a*-value and *b*-value of the GR relationship corresponding to zone 928 were used, which contains the study area. The extrapolation of the GR relationship at magnitude M 4.5 (the maximum magnitude in ZCF2) and M 5.4 (the maximum magnitude in ZCF1) allowed us to obtain $\alpha_2=0.08$ events/year ($\alpha_1=\alpha_2/2$) using the *b*-value of 0.66 reported by the INGV and assuming 400 year for the completeness period (Gruppo di Lavoro MPS 2004). The hazard maps for PGA (in units of *g*, where *g* is the gravity acceleration) for both of the return periods of 475 years and 975 years are shown in Fig. 4. In particular, the left panels in Fig. 4 refer to case #1, while the right panels refer to case #2. Also in Fig. 4, the lower panels refer to the 475-year return period, and the upper panels to the 975-year return period. The results show that as well as the case and return period considered, higher PGA values are

obtained for ZCF2, and that for each single case, PGA increases with the increasing return period. When case #2 is taken into account, the values obtained in the present study for the Campi Flegrei area are in general agreement with the values reported in the Italian national hazard map provided by the INGV (Meletti and Montaldo 2007; Montaldo and Meletti 2007; Spallarossa and Barani 2007). For the whole area, the INGV provides PGA values ranging from 0.150 to 0.170 *g* for the 475-year return period, and from 0.200 to 0.225 *g* for the 975-year return period. The inferred PGA values for case #1 of the present study are, however, significantly lower than those provided by INGV (Meletti and Montaldo 2007; Montaldo and Meletti 2007; Spallarossa and Barani 2007).

Results for the Mt. Vesuvius area

The earthquake source zones, ZVS1 and ZVS2, that were identified on the basis of three historical earthquakes (1861, Mw 4.7; 1631, Mw 5.0; and 1794, Mw 5.0) selected from the CPTI04 catalog (Gruppo di lavoro CPTI 2004) and for recent seismicity are shown in the right panel of Fig. 1. The analysis performed in the present study for both of the seismogenic zones identified was, however, based on a M 3.6 maximum magnitude value, which corresponded to the largest earthquake recorded in the area over the last 65 years, and a M 1.9 minimum magnitude value, which corresponded to the completeness threshold of the seismic catalog (Zollo et al. 2002). In analyses of the seismicity for the period 1972–2000, Zollo et al. (2002) and Del Pezzo et al. (2004) showed decreasing *b*-values from 2.3 to 1.1, which correspond to the present measured value. By extending the same dataset to present times, the mean activity rates for the two zones were estimated: $\alpha_1=37.03$ events/year and $\alpha_2=2.78$ events/year.

The hazard maps for PGA for the 475-year and 975-year return periods and the three selected *b*-values, i.e., 2.3, 1.6 and 1.1, are shown in Fig. 5. These results show that a decrease in the *b*-value for the same range of magnitude, distance and mean activity rate produces an increase in the PGA values for the two earthquake source zones. This is due to the increasing ratio between the numbers of large and small earthquakes. For example, for ZVS1 and the 475-year return period, an estimate of PGA of 0.15 to 0.17 *g* is obtained from the national catalog data (Meletti and Montaldo 2007), while the higher value of 0.45 *g* is predicted using the local catalog data.

Syn-crisis phase

PSHA for the *syn-crisis* phase required some assumptions. In the present analysis, the seismic activity that occurred

during the last 1982–1984 crisis at Campi Flegrei was considered, while for the Mt. Vesuvius area it was arbitrarily assumed that the *syn-crisis* phase has a total duration of 2 years.

PSHA for the phase of interest was performed assuming that the seismicity was characterized by the occurrence of clusters with Poissonian distributions (e.g., De Natale and Zollo 1986) (e.g., generalized Poisson distribution). Given an observation period during which potentially precursory phenomena were observed, peak ground-motion values with a selected return period were then computed. Specifically, the data recorded during the observation period were used to estimate the mean activity rate, the number of earthquakes, and the b -value that provided the input for PSHA. In particular, for each observation period, PSHA was calculated at 6, 12, 18 and 24 months return periods. For the Mt. Vesuvius area, two models for the time dependence of the b -value were tested. Indeed, as reported in various studies, this parameter has been shown to depend on environmental (geological and tectonic) conditions, and its space and time variations are mainly linked to the material properties, the magnitude of applied shear stress, and the temperature gradient (e.g., Wiemer and McNutt 1997; Wyss et al. 1997). As in the example by Marzocchi et al. (2001), an increase in pore pressure due to an increase in heat flux can take the system very close to a critical state, where the seismic activity is very intense and the b -value is high. On the other hand, the seismic activity preceding the 18 May 1980 eruption at Mt. St Helens, and the March 1981 Etna eruption, were characterized by a decreasing b -value (Endo et al. 1981; De Natale et al. 1986). As a consequence, in the present study, models of both a decreasing and an increasing b -value were considered, and their effects on PSHA were analyzed.

Results for the Campi Flegrei area

By using the results of De Natale and Zollo (1986) for the pattern of 1982–1984, an analytic model was derived for both the mean monthly activity rate and the total number of clusters as a function of time. These values were then used to calculate the corresponding b -value. The adopted models and the retrieved coefficients for the mean activity rate $\alpha(t)$ and the total number of clusters $N(t)$ are expressed by the following equations:

$$\alpha(t) = 10^{c_1} t^{c_2} \quad (c_1 = -0.1 \pm 0.1; c_2 = 0.2 \pm 0.1) \quad (4)$$

$$N(t) = 10^{d_1} t^{d_2} \quad (d_1 = 2.4 \pm 0.3; d_2 = 0.3 \pm 0.1) \quad (5)$$

Equations 4 and 5 allow extrapolation of the data for both of the assumed periods of 2 years of unrest. The models reported in Eqs. 4 and 5 are represented in Fig. 6.

PSHA for the Campi Flegrei area was performed assuming $M_{\max}=4.2$ and $M_{\min}=0.6$. As an example, Figs. 7 and 8 show the hazard maps for PGA in units of g for the observation periods of 1 month and 6 months. The results for the longer observation periods, e.g., 12 months and 18 months, did not change substantially as a result of the small variation in the input parameters, as did the seismic activity and b -values after about 10 months. The

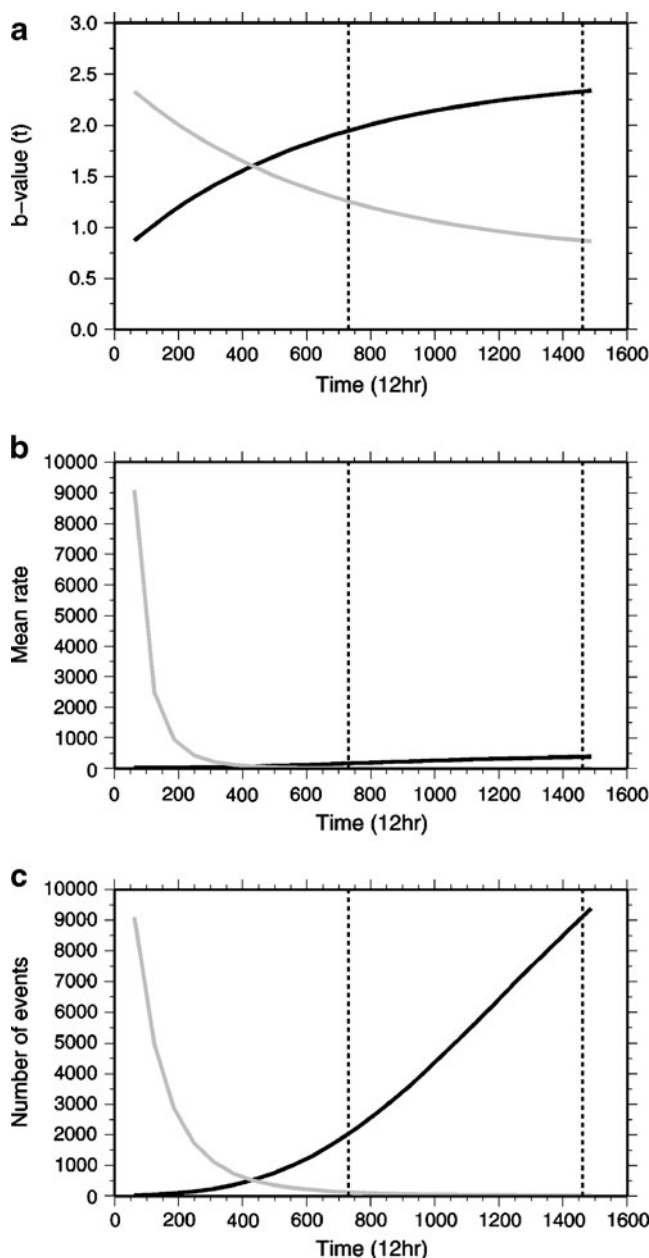


Fig. 9 Seismicity models characterizing the Mt. Vesuvius area during the *syn-crisis* phase. Grey lines, decreasing b -value model. Black lines, increasing b -value model

results obtained show that the highest PGA values are found for ZCF2 (see Fig. 1). In particular, for the 1-month observation period (Fig. 7), the highest PGA value was 0.01 g, which increased to 0.02 g when the 6-month observation period and 24-month return period were taken into account. Moreover, the increase in the observation period was followed by an increase in the extent of the area where higher values were observed.

Results for the Mt. Vesuvius area

No instrumental data exist for the *syn-crisis* phase for the Mt. Vesuvius area, so we performed the calculations

for the opposite cases of time-increasing and time-decreasing *b*-values. Observations at several volcanoes showed time-increasing *b*-values before the eruptions (e.g., Mt. Spurr, Alaska, 1992; Mt Etna, Italy, 1981) (e.g., De Natale et al. 1986), while at Mount St Helens before the 18 May 1980 eruption the *b*-value decreased with time (e.g., Endo et al. 1981). Once the magnitude range *M* (1.9, 3.6) had been selected, the *a*-value of the GR relationship was used to calculate the total number of clusters for the period considered and the mean activity rate α (number of earthquakes/time period considered) to be used in Eq. 1. The models and their corresponding parameters are shown in Fig. 9. For the Mt. Vesuvius

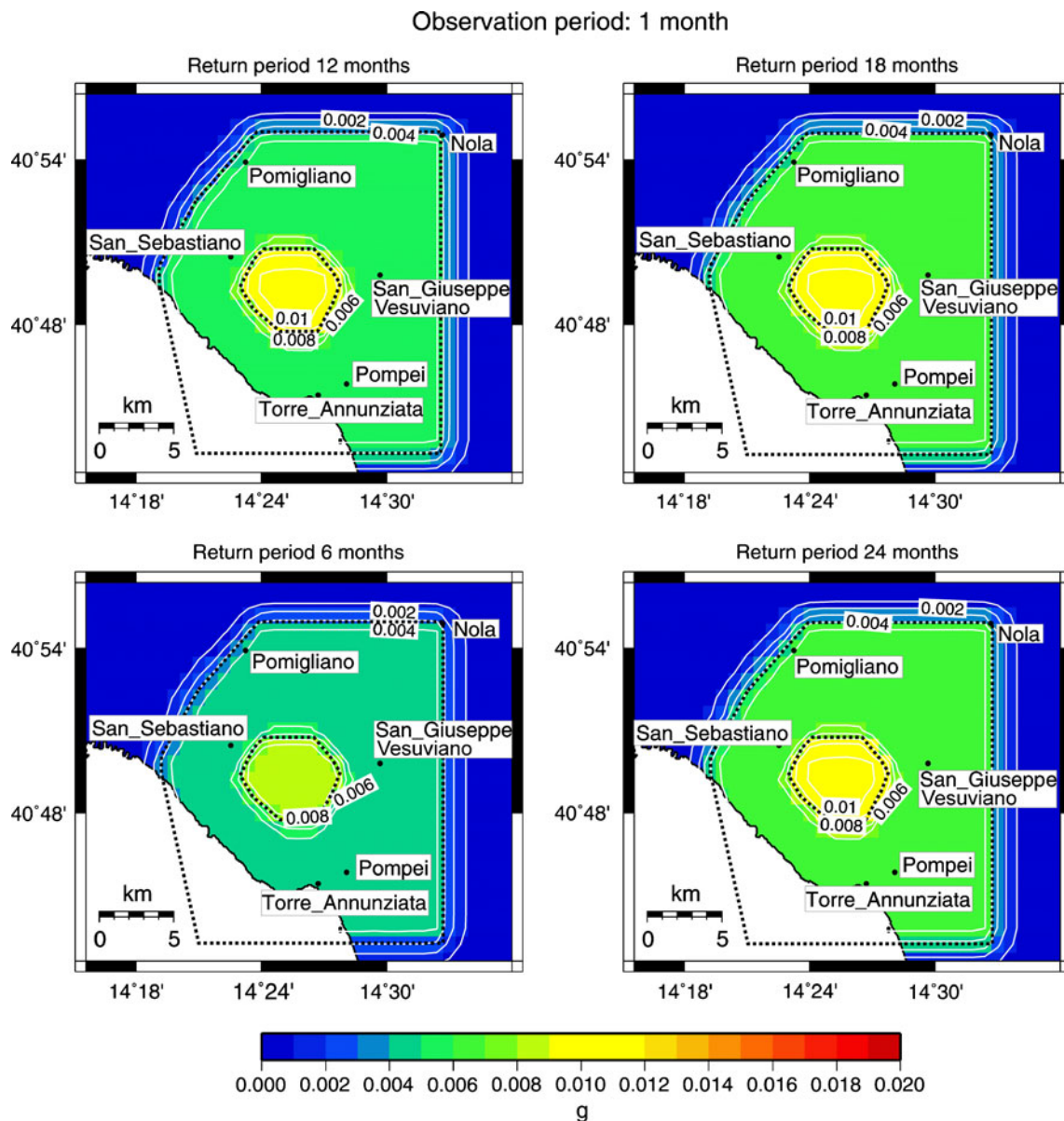


Fig. 10 Hazard maps for PGA expressed in units of *g* for *syn-crisis* phase at the Mt. Vesuvius area relative to the 1-month observation period and decreasing *b*-value models

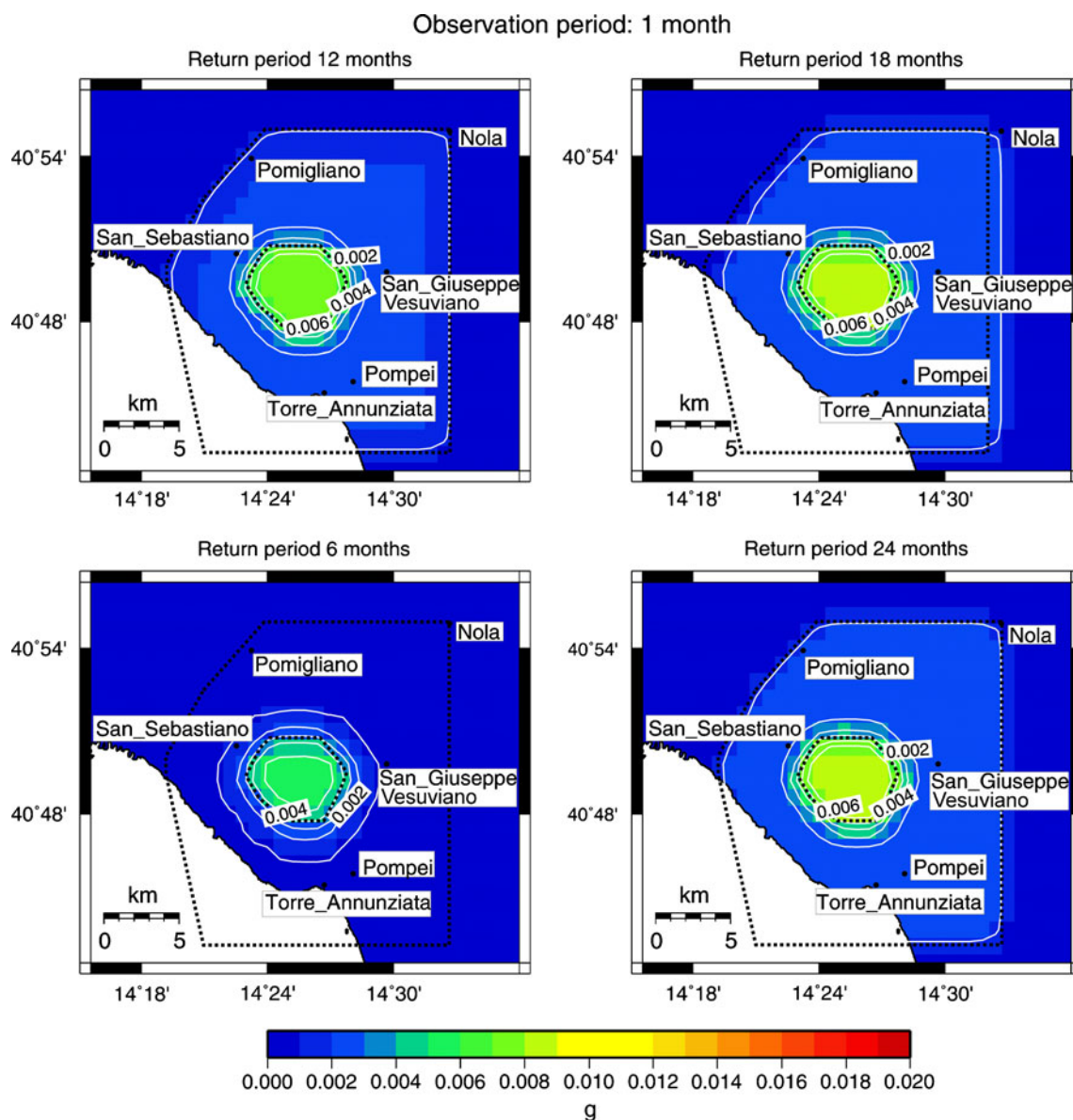


Fig. 11 As for Fig. 10, but for increasing b -value models

area, Figs. 10 and 11 show the hazard maps for PGA in units of g obtained for a 1-month period of data collection, and the same four return periods considered for the Campi Flegrei area. Specifically, Fig. 10 refers to the model of a decreasing b -value with time, while Fig. 11 refers to an increasing b -value with time. The highest PGA values were estimated corresponding to ZVS1 for the case of a decreasing b -value with time to the eruption.

To analyze how these results depended on the observation period, a site-specific analysis was performed. The two sites of SVS1 and SVS2, located in ZVS1 and ZVS2, respectively (see Fig. 1), were selected for extrapolation of the PGA values from the hazard maps calculated at all of

the observation and return periods, and reported in Fig. 12. In particular, for both of these selected sites, the left panels in Fig. 12 refer to the time-decreasing b -values, and the right panels refer to the time-increasing b -values, before the eruption. The results indicate that sites located in ZVS1 were affected by higher hazard values and that the model of the time-decreasing b -values provides higher PGA values, as expected. These differences were more evident for the 12-month and 18-month observation periods. With the time-increasing b -values to the eruptions (Fig. 12, right panel), the SVS1 recorded higher PGA values with respect to SVS2, which, on the contrary, experienced PGA values that were quite constant, independent of the observation and return periods.

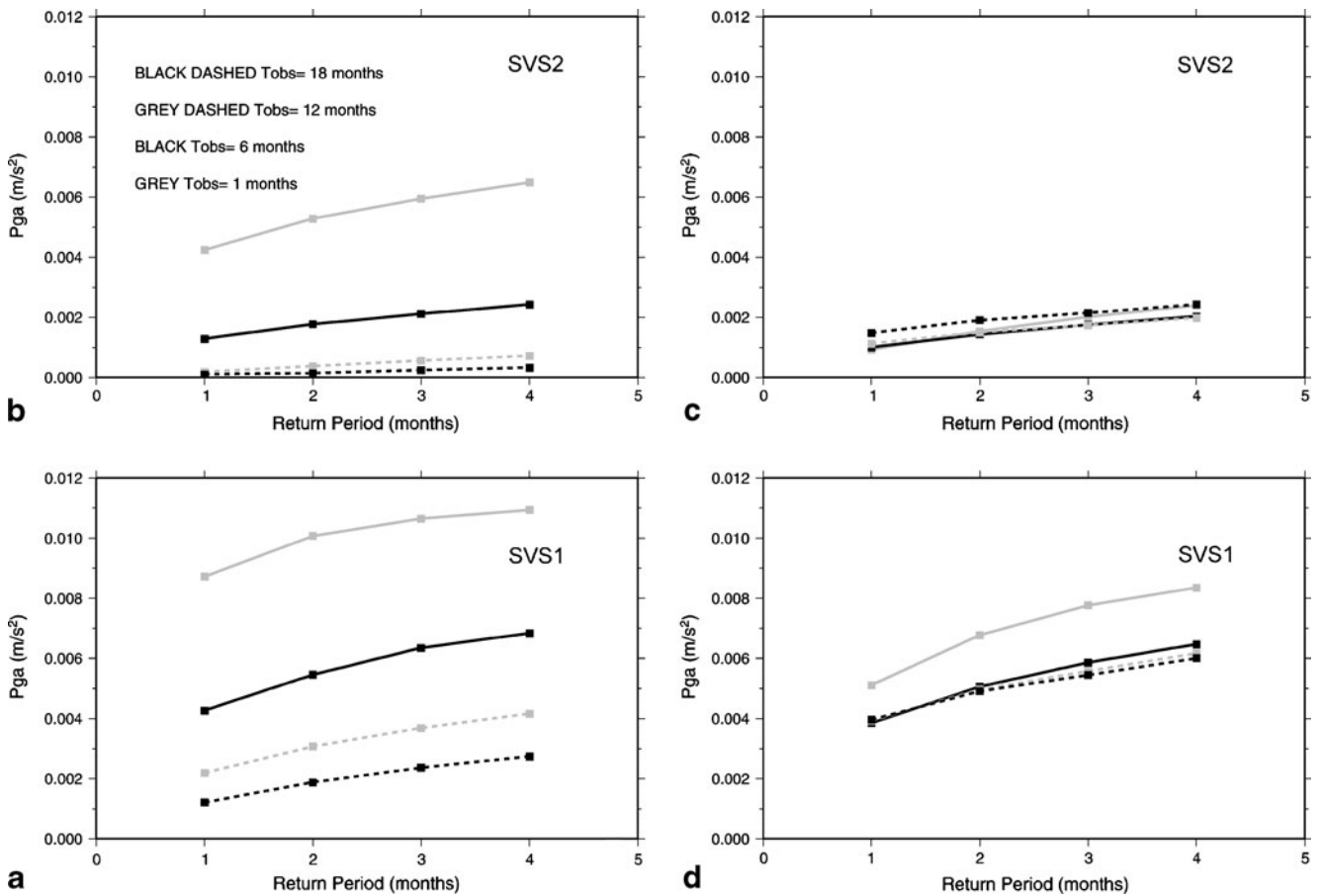


Fig. 12 Hazard values for four observation periods and four return periods. *Left panels, b-value decreasing model. Right panels, b-value increasing model*

The uniform hazard spectra

From an engineering point of view, seismic hazard in terms of PGA values can be of little interest. Indeed, in practice, the elastic response of a structure to earthquake ground motion can be modeled as a simple oscillator whose natural period is the same as that of the structure (Reiter 1990). A large proportion of the civil structures have an elastic period of about 1 s, which requires that spectral ordinates at periods different from zero (corresponding to PGA) should be considered. As a consequence, the most complete hazard assessment is in terms of a uniform hazard spectrum, which is an elastic response spectrum (commonly, 5% critically damped) that is derived from an analysis of the PSHA at the site (e.g., Reiter 1990). Specifically, the UHS is defined with the purpose that all of its spectral ordinates have the same probability of exceedance in a time interval depending on the limit-state of interest that depends on the performance required by the structure in response to the earthquake ground motion (e.g., collapse, safety of life). In practice, once the probability of exceedance has been selected, each point on the spectrum can be obtained by

solving the hazard integral (Eq. 1) for each of the structural periods of interest.

For both of the areas studied, two sites with different locations with respect to the source zones were selected (see Fig. 1) and the time-dependent hazard was computed in terms of $S_a(T)$ for $T=0.0, 0.15, 0.3$ and 1 s. Figure 13 shows the results for the two selected sites in the Campi Flegrei area. In particular, the left panels in Fig. 13 refer to the SCF1 site, and the right panels to the SCF2 site. Each panel also reports the observation periods and the corresponding return periods (T_r). In agreement with the seismicity model considered, which was characterized by low-to-moderate high frequency earthquakes occurring at short distances, for both of the sites, the highest values corresponded to the largest return period, i.e., 24 months and $S_a(T=0.3$ s). On the other hand, for the two sites selected, at the selected observation periods and return periods, the values at $S_a(T=1$ s) are the same, and are slightly different at other's structural periods. This is due to a lack of large distant earthquakes that dominate the UHS at periods of about 1 s or more (Reiter 1990; Convertito et al. 2009).

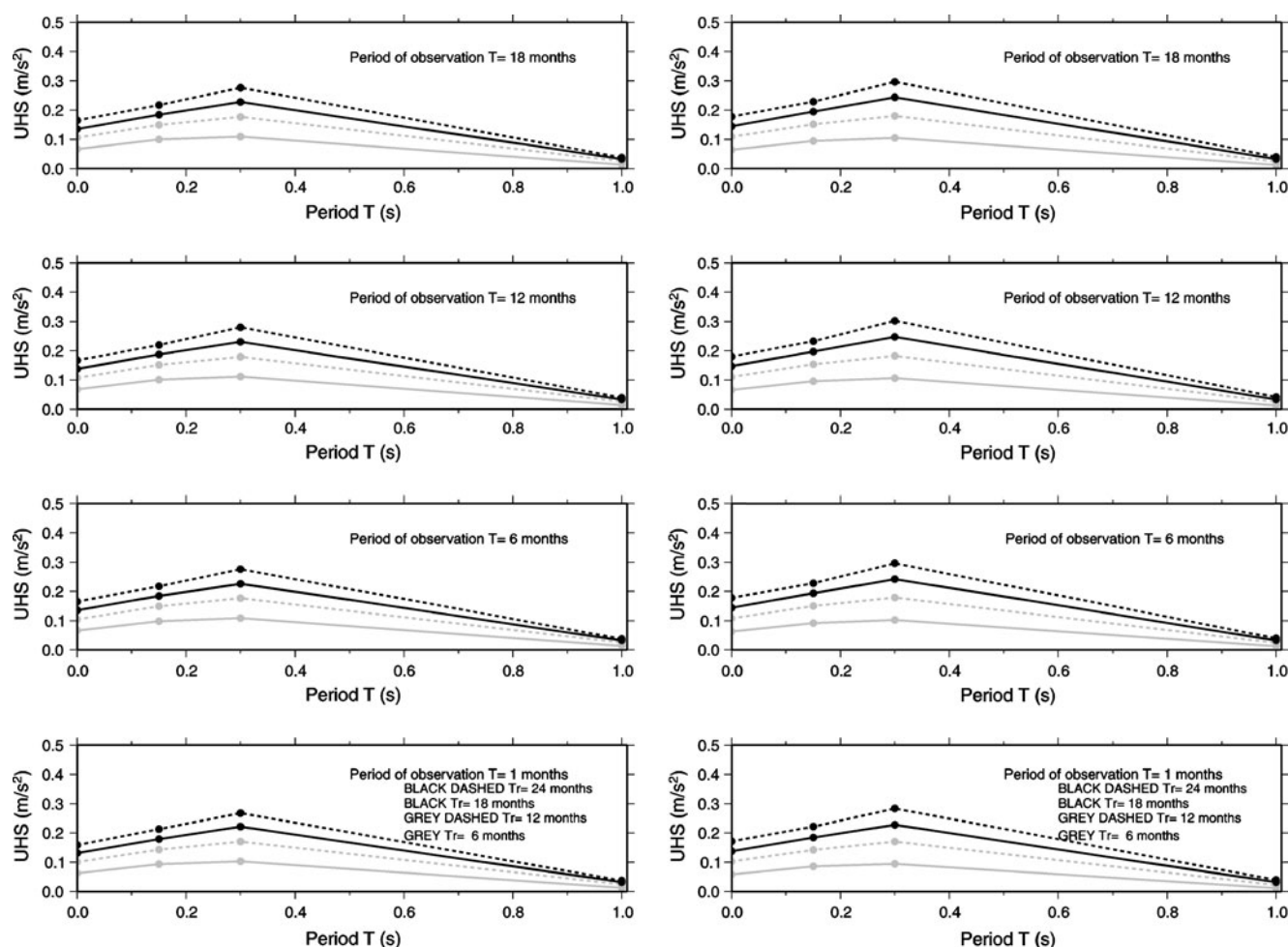


Fig. 13 Uniform hazard spectra for the Campi Flegrei area. *Left panels*, site SCF1. *Right panels*, site SCF2

The two time-dependent b -value models were also investigated for two selected sites in the Mt. Vesuvius area. Figure 14 shows the results for the SVS1 site, and Fig. 15 shows the results for the SVS2 site. In each of Figs. 14 and 15, the left panels refer to the model for the time-decreasing b -values and the right panels to that for time-increasing b -values. For SVS1, when the time-decreasing b -value model is considered, there is large variability in the UHSs for all of the $S_a(T)$, and the largest values correspond to $T=0.3$ s and the 1-month observation period. This can be explained because for the assumed magnitude range, the hazard curves are mainly affected by low-magnitude earthquakes with a high frequency of occurrence, rather than by larger magnitude earthquakes. The SVS2 site shows the same features, but it is characterized by lower values due to its location with respect to the seismic sources. On the other hand, when the time-increasing b -value model was considered, the UHSs did not vary as a function of the observation period, which indicates that from an engineering point of view, the seismicity that characterizes the first

month of activity represents the largest threat during the unrest phase.

Discussion and conclusions

The present study investigated the probabilistic seismic hazard for two volcanoes, Campi Flegrei caldera and Mt. Vesuvius, in the Campania region of southern Italy. For these two areas, earthquake source zones were identified based on both historical earthquakes and recent seismicity. Furthermore, to estimate the effects of the selected earthquakes, ground-motion-prediction equations accounting for the differences in the attenuation features were retrieved at four spectral ordinates. The results presented here do not take into account soil conditions at individual sites, but can be tailored for specific sites if the site-response or amplification coefficients are known.

Two different phases have been considered here: *pre-crisis* and *syn-crisis*. These phases represent the present

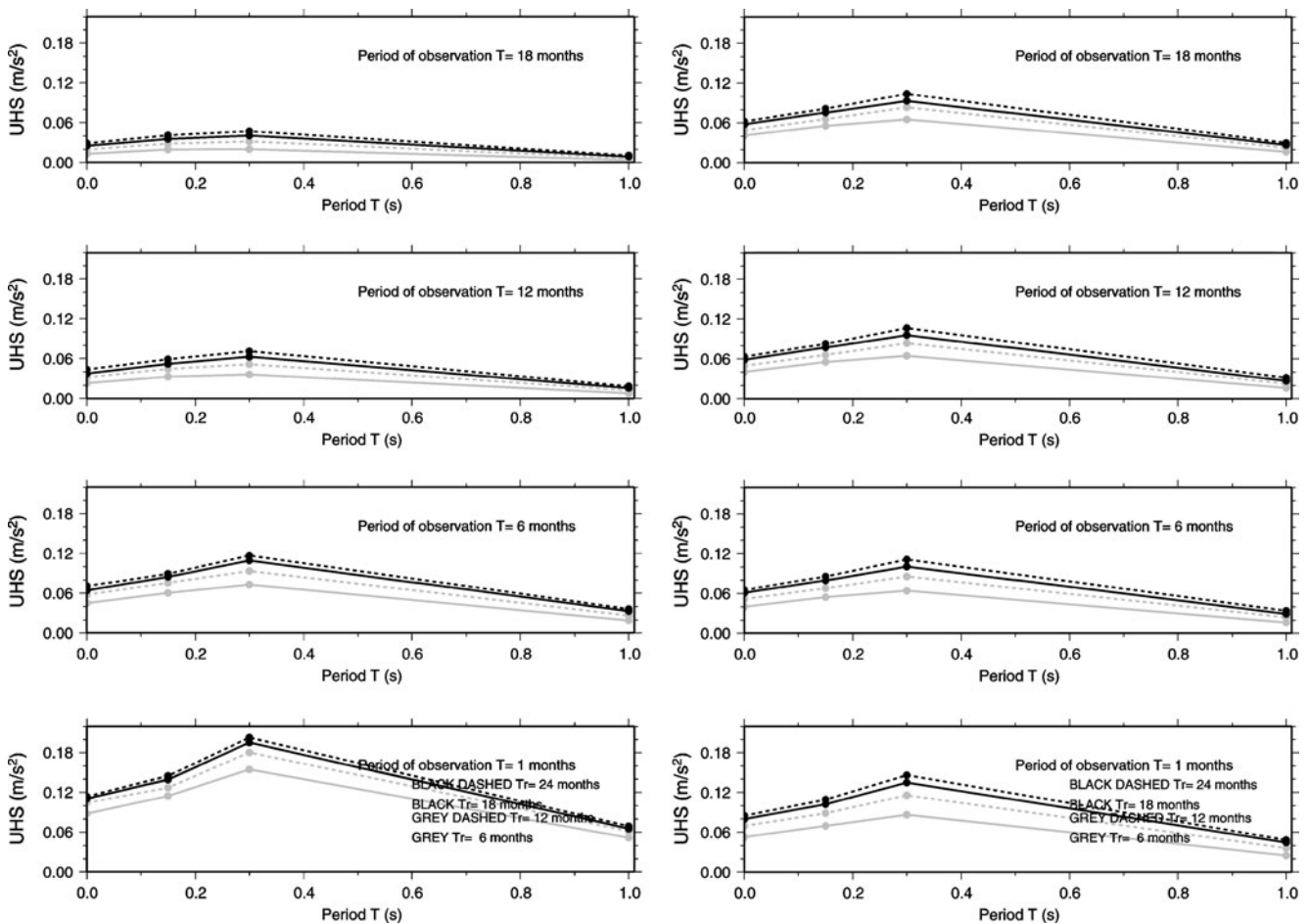


Fig. 14 Uniform hazard spectra for the Mt. Vesuvius area and the SVS1 site. *Left panels*, decreasing b -value model. *Right panels*, increasing b -value model

quiescent state of the volcanoes and the phase of unrest potentially preceding an eruption, respectively.

The results obtained for the *pre-crisis* phase show that:

- For the Campi Flegrei caldera, the results are in general agreement with those provided by standard procedures for Italian national seismic hazard mapping (Meletti and Montaldo 2007; Montaldo and Meletti 2007) when using the same hypotheses for the b -value. On the other hand, when local data are used to calculate the seismicity rate, the PGA values inferred in the present study are significantly lower (~30–40%) than those provided by the currently adopted nation-wide hazard map.
- For Mt. Vesuvius, when the local data are used, the hazard values in terms of PGA are higher (~50%) than those reported in the national hazard map, as a consequence of the magnitude values selected and the decreasing b -value with time. A decreasing b -value produces a higher occurrence of large magnitude earthquakes.

For the *syn-crisis* phase, a total duration of 2 years for the crisis was assumed, as comparable with that of the

1982–1984 crisis that occurred in the Campi Flegrei area. This can be a critical issue, particularly when a decreasing b -value model is assumed. Indeed, in this case, the peak ground-motion prediction obtained from early periods of data collection might be not representative for the full duration of the crisis, due to changes in the ratio between the numbers of large and small earthquakes. On the other hand, as shown by the present study, when an increasing b -value model is assumed, the results obtained from the early period of data observation in terms of UHS, and not only in terms of PGA, are representative for the whole duration of the crisis. The *syn-crisis* phase was analyzed by assuming three different periods of data collection (1, 6, 12 and 18 months) and by estimating the hazard for four return periods (6, 12, 18 and 24 months).

The main results of the analysis for the Campi Flegrei caldera are that:

- The results for longer observation periods, e.g., 12 and 18 months, do not change substantially because there are only small variations in the input parameters, such

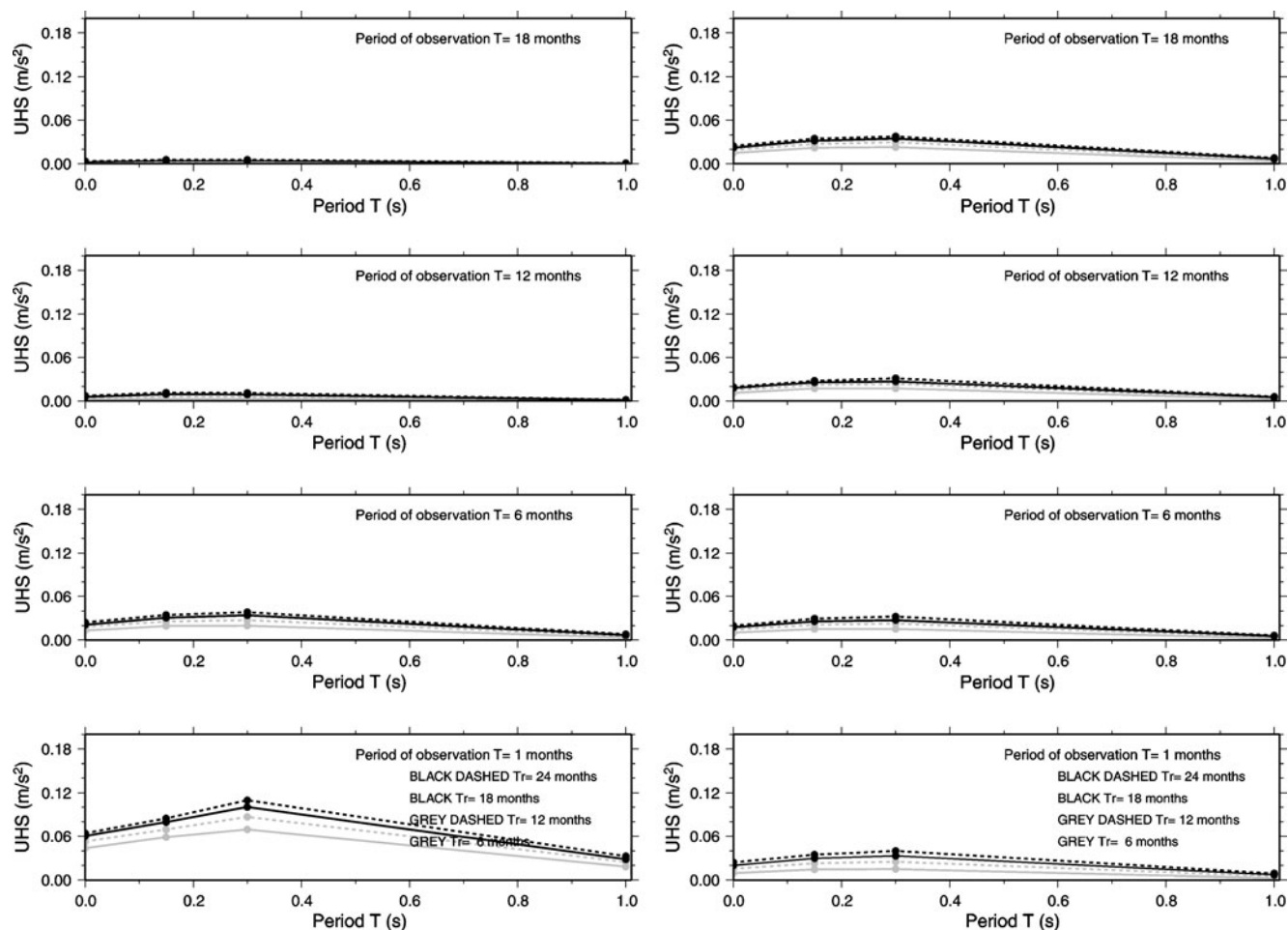


Fig. 15 As for Fig. 14, but for the SVS2 site

as the seismic activity and b -values, after about 10 months.

- The highest PGA values are found for ZCF2 (see Fig. 1). In particular, for a 1-month observation period (Fig. 7), the highest PGA value was 0.01 g , which increased to 0.02 g when the 6-month observation period and 24-month return period were taken into account.
- Increasing the observation period caused an increase in the extent of the area where higher values were observed.
- The results in terms of UHSs show that the highest $S_a(T)$ values are predicted for the largest return period and for the structural period $T=0.3$ s, as a consequence of the assumed seismicity model.

The main results of the analysis for Mt. Vesuvius are that:

- Site-specific analysis indicated that sites located in ZVS1 are characterized by higher hazard values, and that the model predicting a decreasing b -value provides higher PGA values, as expected.
- When the b -value increases with time preceding an eruption, SVS1 recorded higher PGA values with respect to SVS2. The SVS2 site was characterized by

PGA values that were relatively constant, independent of the observation and return periods.

- The analysis performed in terms of UHSs provides different results for the two sites selected and the two b -value models. Specifically, when the time-decreasing b -value model was considered, the SVS1 site experienced a large variability in the UHSs for all of the $S_a(T)$. The largest values corresponded to $T=0.3$ s and a 1-month observation period. The SVS2 site showed the same features, although it was characterized by lower values due to its greater distance from the seismic sources. On the other hand, when the increasing b -value model was considered, the seismicity that characterized the first month of activity was representative of the hazard during the unrest phase.

The results of the present study show the importance of time-dependent hazard calculations of seismic activity in volcanic areas. This analysis should be based on observations and measurements continuously acquired by local seismic networks. It can then be much more informative than a static hazard calculation based on hypotheses concerning only the past activity of the volcanoes.

Additionally, it is worth calculating the hazard in terms of UHS rather than considering only the PGA. Indeed, according to its definition, UHS provides a full descriptive image of the effects of the time-evolving seismicity on the engineering structures, both in terms of magnitude and distance, and can correlate much more closely with expected damage.

Acknowledgments This study was supported by the Italian *Dipartimento della Protezione Civile* as part of the Progetto INGV-DPC V5 SPEED (2007–2009). Scenari di scuotimento in aree di interesse prioritario e/o strategico TASK 1. PERICOLOSITÀ CONNESSA A TERREMOTI PRE E SIN ERUTTIVI: Valutazione dell'Hazard sismico nelle aree vulcaniche Vesuvio e Campi Flegrei. The development of a method for time-dependent seismic hazard due to natural seismicity has been partly supported by the FP7 EU research project Geiser-Geothermal Engineering Integrating Mitigation of induced seismicity in reservoirs. The authors wish to thank Prof. Edoardo Del Pezzo, an anonymous reviewer, and the associate editor Dr. Maurizio Ripepe, whose helpful comments greatly improved the clarity and quality of the manuscript. The Figures were prepared with Generic Mapping Tools (Wessel and Smith 1991).

References

- Ambraseys NN, Simpson KA, Bommer JJ (1996) Prediction of horizontal response spectra in Europe. *Earthq Eng Struct Dyn* 25:371–400
- Anderson JG, Hough SE (1984) A model for the shape of the Fourier amplitude spectrum acceleration at high frequencies. *Bull Seismol Soc Am* 74:1969–1993
- Battaglia J, Zollo A, Virieux J, Dello Iacono D (2008) Merging active and passive data sets in traveltome tomography: the case study of Campi Flegrei caldera (Southern Italy). *Geophys Prospect* 56:555–573. doi:10.1111/j.1365-2478.2007.00687.x
- Bazzurro P, Cornell CA (1999) Disaggregation of seismic hazard. *Bull Seismol Soc Am* 89:501–520
- Boore DM (1983) Stochastic simulation of high-frequency ground motion based on seismological models of the radiated spectra. *Bull Seismol Soc Am* 73:1865–1893
- Campbell KW (1981) Near-source attenuation of peak horizontal acceleration. *Bull Seismol Soc Am* 71:2039–2070
- CEN, European Committee for Standardisation TC250/SC8(2003) Eurocode 8: design provisions for earthquake resistance of structures, Part 1.1: General rules, seismic actions and rules for buildings, PrEN1998-1
- Chen WF, Scawthorn C (2003) *Earthquake engineering handbook*. CRC Press LLC, Florida
- Convertito V, Iervolino I, Herrero A (2009) Importance of mapping design earthquakes: insights for the Southern Apennines, Italy. *Bull Seismol Soc Am* 99:2979–2991. doi:10.1785/0120080272
- Cornell CA (1968) Engineering seismic risk analysis. *Bull Seismol Soc Am* 58:1583–1606
- Corrado G, Guerra I, Lo Bascio A, Luongo G, Rampoldi R (1976) Inflation and microearthquake activity of Phlegraen Fields, Italy. *Bull Volcanol* 40:169–188
- De Natale G, Zollo A (1986) Statistical analysis and clustering features of the Phlegraen fields earthquake sequence (May 1983–May 1984). *Bull Seismol Soc Am* 76:801–814
- De Natale G, Gresta S, Patané G, Zollo A (1986) Statistical analysis of earthquake activity at Etna volcano (March 1981 eruption). *Pure Appl Geophys* 123:697–705
- De Natale G, Iannaccone G, Martini M, Zollo A (1987) Seismic sources and attenuation properties at Campi Flegrei volcanic area. *Pure Appl Geophys* 125:883–917
- Del Pezzo E, De Natale G, Zollo A (1984) Space-time distribution of small earthquakes at Phlegraen Fields, Southern-central Italy. *Bull Volcanol* 47:201–207
- Del Pezzo E, Bianco F, Saccorotti G (2004) Seismic source dynamics at Vesuvius volcano, Italy. *J Volcanol Geotherm Res* 133:23–39
- Endo ET, Malone SD, Noson LL, Weaver CS (1981) Locations, magnitudes, and statistics of the March 20–May 18 earthquake sequence. *US Geol Surv Profess Paper* 1250:93–107, Washington, DC
- Galluzzo D, Del Pezzo E, La Rocca M, Castellano M, Bianco F (2009) Source scaling and site effects at Vesuvius volcano. *Bull Seismol Soc Am* 99:1705–1719
- Giardini D (Editor) (1999) The Global seismic hazard assessment program (GSHAP) 1992–1999. *Ann Geofis* 42:957–1230
- Gruppo di lavoro CPTI (2004) *Catalogo Parametrico dei Terremoti Italiani, versione 2004 (CPTI04)*. INGV, Bologna
- Gruppo di Lavoro MPS (2004) *Redazione della mappa di pericolosità sismica prevista dall'Ordinanza PCM 3274 del 20 marzo 2003. Rapporto Conclusivo per il Dipartimento della Protezione Civile, INGV, Milano-Roma, aprile 2004, 65 pp. + 5 appendici*
- Gutenberg B, Richter CR (1944) Frequency of earthquakes in California. *Bull Seismol Soc Am* 34:185–188
- Marzocchi W, Vilardo G, Hill DP, Ricciardi GP, Ricco C (2001) Common features and peculiarities of the seismic activity at Phlegraen fields, Long Valley, and Vesuvius. *Bull Seismol Soc Am* 91:191–205
- Meletti C, Montaldo V (2007) Stime di pericolosità sismica per diverse probabilità di superamento in 50 anni: valori di ag, Progetto DPC-INGV S1, Deliverable D2. <http://esse1.mi.ingv.it/d2.html>. Accessed 20 January 2010
- Meletti C, Galadini F, Valensise G, Stucchi M, Basili R, Barba S, Vannucci G, Boschi E (2008) A seismic source zone model for the seismic hazard assessment of the Italian territory. *Tectonophysics* 450:85–108
- Montaldo V, Meletti C (2007) Valutazione del valore della ordinata spettrale a 1 sec e ad altri periodi di interesse ingegneristico, Progetto DPC-INGV S1, Deliverable D3. <http://esse1.mi.ingv.it/d3.html> (in Italian)
- Newhall CG (2009) *Volcanology 101 for Seismologists*. In: Schubert G, Kanamori H (eds) *Earthquake seismology*. Elsevier, Amsterdam, pp 351–388
- Qamar A, ST LW, Moore JN, Kendrick G (1983) Seismic signals preceding the explosive eruption of Mount St. Helens, Washington, on 18 May 1980. *Bull Seismol Soc Am* 73:1797–1813
- Reiter L (1990) *Earthquake hazard analysis*. Columbia University Press, New York
- Sabetta F, Pugliese A (1996) Estimation of response spectra and simulation of non stationary earthquake ground motion. *Bull Seismol Soc Am* 86:337–352
- Spallarossa D, Barani S (2007) Disaggregazione della pericolosità sismica in termini di M-R-ε, Progetto DPC-INGV S1, Deliverable D14. [<http://esse1.mi.ingv.it/d14.html>] (in Italian)
- Wessel P, Smith WHF (1991) Free software helps map and display data. *EOS Trans Am Geophys Union* 72:445–446
- Wiemer S, McNutt SR (1997) Variations in the frequency-magnitude distribution with depth in two volcanic areas: Mount St. Helens, Washington, and Mt. Spurr, Alaska. *Geophys Res Lett* 24:189–192
- Wyss M, Shimazaki K, Wiemer S (1997) Mapping active magma chambers by b values beneath the off-Ito volcano, Japan. *J Geophys Res* 102:413–422
- Zollo A, Marzocchi W, Capuano P, Lomax A, Iannaccone G (2002) Space and time behavior of seismic activity at Mt. Vesuvius Volcano, Southern Italy. *Bull Seismol Soc Am* 92:625–640